JOURNAL OF NEUROPHYSIOLOGY
Vol. 41, No. 6, November 1978. *Printed in U.S.A.*

Properties of Concentrically Organized X and Y Ganglion Cells of Macaque Retina

F. M. DE MONASTERIO

Section of Physiology, Laboratory of Vision Research, National Eye Institute, National Institutes of Health, Bethesda, Maryland 20014

SUMMARY AND CONCLUSIONS

1. Macaque retinal ganglion cells having concentrically organized receptive fields were classified as X- or Y-cells on the basis of the linearity or nonlinearity of their spatial summation to a "null" test of alternating contrast and drifting gratings.

2. When an alternating-phase bipartite field positioned at the middle of the receptive field was used as a stimulus, X-cells had a null position, whereas Y-cells showed a doubling of the response frequency. When drifting sine-wave gratings of low contrast were used as a stimulus, X-cells showed a periodic modulation of their discharge having the same mean value for different spatial frequencies, whereas Y-cells showed a large increase in the mean value of their discharges.

3. X-cells had opponent-color responses that received cone-specific signals, i.e., center and surround responses were mediated by input from spectrally different types of cone, whereas Y-cells had broad-band spectral responses receiving mixed-cone signals, i.e., center and surround responses were totally or partly mediated by input from the same type(s) of cone. In most Y-cells, the spatially opponent responses from the center and the surround were mediated by the same types of cone and were thus spectrally nonopponent; other Y-cells showed spectral opponency, since one of the types of cone mediating responses of one region of the receptive field (e.g., center) was absent in the responses of the other region (e.g., surround).

4. X- and Y-cells projected to the lateral geniculate body. Opponent-color X- and Y-cells did not project to the superior colliculus, whereas a fraction of spectrally nonopponent Y-cells projected to this structure.

5. X-cells tended to have longer conduction latencies, less transient responses to small stimuli, and a more central retinal distribution than Y-cells; these differences, however, represented tendencies and not invariant properties.

6. The results show that the X/Y dichotomy of ganglion cells is present in the retina of macaques and indicate that the degree of the linearity of spatial summation of incoming cone signals to the cells is related to the degree of cone specificity of spectral inputs to the receptive-field mechanisms.

INTRODUCTION

Over the last years, a distinction between two systems involving neurons generally known as X- and Y-cells has become prominent in the visual system of vertebrates. The discovery in the cat retina of an X/Y dichotomy of ganglion cells (16), independent of the on-center/off-center dichotomy of Kuffler (20), has provided the basis for most suggestions on the parallel processing of visual information that are currently in vogue. By using a grating presumably occupying the entire receptive field, Enroth-Cugell and Robson (16) noted on reversing the contrast of the grating that in some cells (X) a position could be found in which no significant responses were elicited when the dark and light bars were exchanged, whereas in other cells (Y) no such null position could be found. This finding indicated that incoming photoreceptor signals to an X-cell were

Received for publication March 14, 1978.

linearly summed within the center and within the surround mechanisms, while incoming signals to a Y-cell were nonlinearly summed.

Until recently there has been no clear indication of an X/Y dichotomy in the primate visual system, where several functionally distinct cell types have been described. Wiesel and Hubel (27) divided neurons in the lateral geniculate body into four cell types on the basis of their degrees of spatial and spectral opponency and their laminar segregation. Recent geniculate studies (14, 21), principally based on classificatory criteria other than the original X/Y one, have indicated the presence of an X-like/Y-like dichotomy of neurons. At the retinal level, three main classes of ganglion cells have been described, encompassing the four geniculate cell types and containing a few other new cell types (9, 23). Preliminary results have suggested that cells of two of these groups may correspond to X- and Y-cells on the basis of the degree of linearity of spatial summation (12), and it has been suggested that similar cell types can also be distinguished on the basis of their spectral opponency, conduction latencies, and response waveform (23). The putative X/Y dichotomy of the macaque retina and lateral geniculate body bears on primate color vision. In general, the indications are that the retinal dichotomy appears to be related to the presence or absence of opponent-color responses (23). At the geniculate level there are some conflicting reports (14, 21), although ambiguities and different criteria make it difficult to ascertain the homology of the classifications.

The present paper and the following one (7) describe the functional properties of X and Y macaque ganglion cells having a center-surround organization whose spatial and spectral properties are similar to those of types I, III, and IV of the lateral geniculate body (27), whereas a third paper (8) describes functional properties of ganglion cells lacking a typical center-surround organization (type II and other cell classes). In addition to extending the X/Y dichotomy to the macaque retina, the results provide evidence that the degree of linearity of the spatial summation of incoming (cone) signals to the center and surround mechanisms of the cells is related to the degree of cone specificity of these signals, rather than simply to the presence or absence of opponent-color responses.

METHODS

Intraocular recordings from ganglion cells were obtained in the retina of juvenile rhesus and cynomolgus monkeys anesthetized with sodium pentobarbital (1.5–5 mg/kg·h) or, occasionally, ketamine hydrochloride (5–20 mg/kg·h) administered with a 5% dextrose-lactate-Ringer solution in a continuous intravenous or intra-arterial infusion. The animals were paralyzed with a continuous infusion of gallamine triethiodide (15–20 mg/kg·h) and *d*-tubocurarine (0.3–0.5 mg/kg·h) and were artificially respired (20–25 strokes/min, 25–35 ml/stroke). Rectal temperature (36–37°C), mean arterial femoral pressure (80–90 mm Hg), and expired end-tidal CO_2 (4–5%) were monitored and maintained within normal limits; ECG rate and waveform, cortical EEG, and urine output were also continuously monitored. Hematocrit measurements were taken daily; high values (≧40%) were corrected by increasing the amount of saline infusion, whereas low values were corrected with diuretics. Arterial blood gases were occasionally measured. To avoid the cumulative effects of fixed doses of anesthetic over the 4–5 days the experiments lasted, dosages were adjusted to satisfy the following criteria: *1*) tachycardia and transient hypertension to noxious stimuli, and *2*) cortical EEG recordings (posterior temporal-occipital derivation) with a low-amplitude combination of fast and slow waves smaller than 150–200 μV, typical of a transition between stage I and stage II anesthesia. Nonparalyzed animals showed brisk reflexes but no organized mass responses to noxious stimuli and had smooth eye movements interspersed with saccades to vestibular stimulation by manual head rotation. In these conditions, the animals were accomodated by about 1.5–2 diopters and their pupils were normal in size and reactive to light. Neuromuscular blockade was interrupted at the end of the recording session and resumed prior to the following one. Penicillin was given for 1.5–2 days, while dexamethasone phosphate was given daily (0.5–1 mg). Ipsilateral pneumothorax and urethral catheterization were routinely performed; occasionally, a trocar was inserted into the cisterna magna to allow depressurization, which helped to reduce vascular pulsations. The vagosympathetic trunk and the carotid sheath of some animals were sectioned. Mydriasis and cycloplegia were obtained with cyclopentolate and phenylephrine hydrochloride. A transparent contact scleral lens protected the cornea and a buffered isotonic solution was used for lens cushioning; the contact lens was clipped at both

canthi to permit the introduction of microelectrodes and the mounting of a small mirror glued to the sclera behind the limbus, which reflected a very narrow beam from a He-Ne laser used to monitor eye movements.

A high-pressure, DC xenon arc lamp (150 W, correlated color temperature of ca. 6,000 K) was used as a light source. Stimuli from three independent beams could be presented to the eye in Maxwellian view through a modified fundus camera. The angle of light incidence onto the retina was kept normal by projecting the stimuli through the center of the pupil. No artificial pupil was used as all light entering the eye was contained in a narrow, convergent beam of about 1.2 mm at the cornea. Rectangular pulses of light were obtained from galvanometer-driven flag shutters placed at focal points of the light beams. Small apertures with thin pieces of frosted glass were mounted in front of the condenser system of the lamp so that the arc but not the lamp electrodes served as the radiant source; this provided a very homogeneous output of small angular subtense. The output was restricted to the 390- to 700-nm band by appropriate infrared and ultraviolet barrier filters, and it had a spectral flatness of about ±0.15 log units between 400 and 680 nm. The source radiance was monitored with a photometer whose output was continuously monitored; fluctuations with a standard deviation of ca. 0.1 log unit occurred occasionally and were compensated in threshold measurements. Small variations in the position of the plasm of the arc were minimized by using a Gaussian field parallel to the lamp electrodes. Field stops of appropriate size and shape were interposed in the collimated segments of two beams and provided test and background stimuli in the nominal range of 0.01 and 20°. The distance between these stops and the first collecting lens of the fundus camera depended on the state of refraction of the eye after mydriasis and cycloplegia (26). Test and background stimuli could be independently presented, varied in size and shape, and displaced in relation to one another with micrometer drives.

The degree of linearity of spatial summation was examined with a rectangular bipartite field in which the luminance of the halves was reversed in antiphase with either sine- or square-wave modulation using a three-polarizer arrangement (12). The boundary between the halves had a nominal width of 0.009° and both halves had the same size irrespective of the total size of the pattern, which could be varied between 0.08 and 8° by means of a rectangular diaphragm. The mean luminance of the bipartite field was kept constant during contrast reversal at about 1 log unit above cell threshold (measured with flashing stimuli of the same mean luminance) and the difference between the maximal and minimal luminance of each half was about 0.6 log unit. The field halves were polarized at right angles of one another; small differences between the mean luminance of each half due to polarization by reflection were appropriately compensated. For receptive fields located within the central 10°, the orientation of the orthogonal planes of polarization of the stimulus was varied until the independent presentation of each half elicited responses at the same threshold criterion; this avoided dichroic effects caused by the macular pigment (13). A Cornu depolarizer (Melles Griot) was used to remove a small linear polarization component of the light source. The temporal frequency of contrast reversal was kept between 1 and 2 Hz. Sinusoidal gratings drifting in one direction of motion were obtained by projecting through the fundus camera photographic transparencies of sinusoidal gratings, which were moved back and forth in a direction perpendicular to their bars by means of a rectilinear galvanometer driven by a triggerable waveform generator (triangular-wave output). The drift frequency was held at 5 Hz and responses to these stimuli were always recorded for a single direction of motion and in phase-locked conditions. These transparencies were photographed in an oscilloscope displaying gratings with little harmonic distortion at a contrast as high as 90%; the product gamma of negative (Kodak RAR2498) and positive (Kodak fine-grain release positive 5302) development was close to 1.0; the resultant gratings had a mean transmittance of about 20% and a contrast of about 60%.

Near monochromatic light in the 400- to 680-nm band was obtained with narrow-band interference filters (Melles Griot) having a full bandwidth at half-maximum of 10 ± 2 nm and a peak transmission of 50% or more; spectrophotometric examinations revealed absence of secondary transmission bands in the visible spectrum. Monochromatic light irradiance was measured at the plane of the cornea with a reverse-bias photodiode (United Detector Technology). White light was measured with a S.E.I. photometer calibrated in relation to a standard source and retinal illumination was estimated by the method described by Westheimer (26) for Maxwellian view systems. Neutral-density filters were selected with a spectrophotometer for a density flat within ± 0.03 log units in the 400- to 700-nm band; these filters were calibrated in situ with the photodiode, and multiple reflection errors have been corrected in all threshold measurements. Axial and lateral chromatic aberration was estimated by the fundal photographic measurements of various stimuli of different wavelength and size projected onto the retina; chromatic aberration effects at each wavelength could be compensated by appropriate micrometric displacements of a given field stop

along the axial and orthogonal lateral axes of the light beam in relation to the first focal plane of the fundus camera. In practice, however, average compensation settings for the same eye were only used when the stimulus wavelengths were separated by more than 50 nm. Except for the smallest stimuli, the observer could monitor the optical quality of the stimuli and of the fundal image through the fundus camera and introduce the appropriate corrections.

Single-cell activity, usually extracellular, was recorded with glass micropipettes, 25–100 MΩ in the vitreous humor (3 M CH_3COOK), which were introduced into the eye through a closed-chamber system that minimized vitread leakage and firmly anchored the eyeball. The indifferent electrode was located in the vitreous humor. Action potentials were amplified and displayed in a conventional manner. In addition, filtered action potentials triggered an oscilloscope whose gate output was used to generate 0.5- to 1.5-ms pulses put into a CAT 400A computer (400 bins, 2.5 ms each). Responses to incremental stimuli were averaged over 30 presentations and plotted as "pulse-density tracings" (16) with a time constant of 20-50 ms. The waveform of action potentials was monitored in fast-sweep oscillograms to insure single-cell recordings. Unless otherwise stated, functional properties were examined in cell-body recordings. Threshold stimulus intensities were determined as the minimally discernible change in cell firing in about 50% of 10–20 trials; more precise threshold measurements were obtained by averaging 30 trials at each energy level of the stimulus in a double-staircase procedure until a minimally discernible change in the maintained discharge of the cells could be detected in pulse-density tracings. All threshold measurements were taken at the corneal level; the reciprocal of threshold is referred to as sensitivity. Bipolar stimulating-electrode pairs were stereotaxically implanted in both optic tracts, lateral geniculate body, and superior colliculus until mass responses to diffuse light stimulation could be recorded with each one of these electrodes; the more posterior geniculate electrode pair was kept more superficial. Antidromic ganglion cell responses were obtained by passing 1.5-ms pulses (0.5–3 mA) from a constant-current source, and all conduction latencies were measured at 1.5× current threshold. The distance between the recording electrode and the optic tract pairs of electrode varied between 14 and 29 mm, depending on the retinal location of the cell and the side of the central projection of its axon (ipsilateral or contralateral).

For brevity, the terms blue, green, and red cones refer to the cone types having maximal sensitivity in the 440- to 450-nm, 530- to 540-nm, and 570- to 580-nm bands; terms such as red-center, green-surround describe the cone inputs to the opponent regions of the receptive field of the cells, which were determined by the test spectral sensitivity of cell responses on neutral and several colored backgrounds.

RESULTS

The functional properties of 377 ganglion cells located within the central 20° of retinal eccentricity were examined in enough detail and uniform conditions to permit their comparison. All of the cells had a center-surround organization (7), similar to that described by Kuffler (20), and three different types could be distinguished on the basis of the degree of spectral opponency of cell responses. These three types (I, III, and IV) were similar to those described in the lateral geniculate body of macaques (27).

Spectral properties

Type I cells included most of the opponent-color neurons of the sample (57%, 215/377). They received signals from two or three spectrally different cone types and a characteristic feature of these cells was that their center and surround responses were cone specific; i.e., center responses were mediated by signals from a cone type spectrally different from the one(s) mediating surround responses (e.g., green-center, red-surround). Several classes of cone-specific arrangements were observed and these were similar to those listed in Table 1 of de Monasterio and Gouras (9). Many of the properties of type I cells have been described in other studies (9–11) and the present results essentially confirmed previous descriptions. In about 20% of the neurons, typically perifoveal red-center, surround responses were too weak to be detected in the absence of selective light adaptation of center responses (11); no blue-center cells showed such concealment of color and spatial antagonism. Whereas about 70% of the cells appeared to receive input exclusively from green and red cones, the remaining cells, commonly located toward the extrafoveal retina, received input from all three cone types. The varieties and relative incidence of such trichromatic opponent cells were similar to those reported in a previous study (12); characteristically, blue-cone input to the receptive-field center of these cells was never accompanied by input from another

cone type and, in all instances, blue-cone input to the neurons was associated with a trichromatic organization.

Type IV cells (9%, 34/377) included the remaining opponent-color cells of the sample. They received input from two or three different cone types and, differently from the previous cell type, their center and surround responses were cone mixed, i.e., both responses were partly mediated by the same type(s) of cone. In most cells, signals from one of the two or three cone types mediating center responses were absent in the responses from the surround (e.g., red-green-center, red-surround); the reverse arrangement was found in few other cells (e.g., green-center, red-green-surround). The former arrangement received contribution of blue-cone signals to both opponent responses. In all cases, however, the surround mechanism always received input from red cones and these neurons resembled an apparently less-typical geniculate type IV configuration (see Fig. 21B of Ref. 27). Whereas the spectral opponency of type I cells has been described in detail in other studies (e.g., Refs. 9, 17, 27), that of type IV cells is less well known. At least at the retinal level, the chromatic unbalance of cone signals to type IV cells results in broad-band spectral opponency (most noticeable with but not restricted to large stimuli), since different wavelengths produce opposite responses and these can be modified by selective chromatic adaptation.

Figure 1 illustrates these properties in a type IV cell whose center received input from all three cone types while its surround received input from blue and red cones (e.g., Fig. 12 of Ref. 9). On a white background (W), midspectral and short wavelengths elicited on-responses of different time courses, whereas long wavelengths elicited both on- and off-responses in addition to an obviously delayed inhibition of on-responses. A 480-nm background (B) increased off-responses to long wavelengths and produced more sustained on-responses to short wavelengths, whereas a 660-nm background (R) produced the opposite effect. The latter and a 580-nm background (Y) also revealed prominent off-responses to short wavelengths, which were not present on white or blue backgrounds. In the presence of a combined 440- and 640-nm background (M), which adapted the red-cone and blue-cone input to the cell, responses to all wavelengths were restricted to the on-phase of the incremental stimulus and no off-responses were elicited, indicating that the former were mediated by green-cone input; these on-responses could be elicited with the smallest spots, indicating that they were generated from the receptive-field center, whereas the off-responses required larger stimuli, indicating that they were generated from the surround. Similar responses to midspectral and long wavelengths were obtained in other type IV cells lacking input from blue cones. Thus, the spectral opponency of type IV was not only manifested in terms of excitation and inhibition competing in the same phase of the stimulus cycle, as in the case of type I cells (7, 9), but also in terms of excitation at different phases of the cycle (7).

Type III cells (34%, 128/377) had center and surround responses receiving input from the same cone types, almost exclusively red and green cones, and thus had a broad-band spectral sensitivity but lacked spectrally opponent properties. About 6% of these neurons had surround responses too weak to be detected in the absence of light-adaptation of the center, resembling "surround-concealing" ganglion cells of the cat (15); these neurons were the achromatic counterpart of some perifoveal type I cells (11). Center and (disclosed) surround responses had similar test spectral sensitivities peaking at midspectral wavelengths; the weakness of surround antagonism resulted in responses to a small spot and a large spot being more sustained than those of more typical type III cells. In contrast, a few cells located within the foveal region had powerful surround antagonism of center responses which resulted in extremely transient activity during the presentation of most stimuli (see below).

Nonopponent-color ganglion cells of this type have been reported to lack input from blue cones (17); the present results, however, suggest that a fraction of these cells received weak input from these cones. Figure 2 (top) shows action spectra of a type III cell on white and monochromatic backgrounds. This cell had a typical center-surround antagonism, as shown by the higher sensitivity of responses to a small spot (open circles) than to a larger one (solid

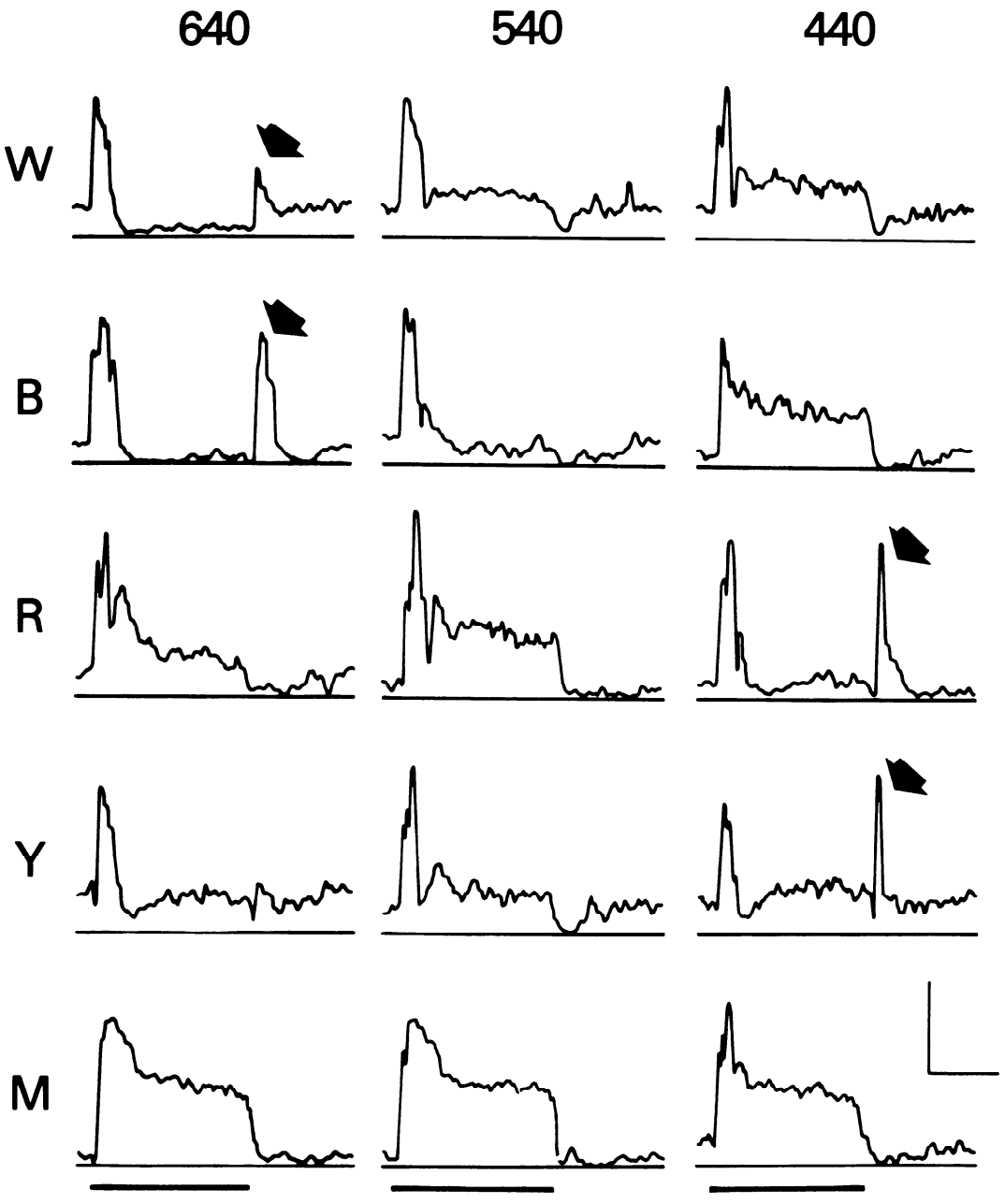

FIG. 1. Responses of a type IV cell whose center received input from all three cone types and whose surround received input from blue and red cones. Stimulus of 0.4° arc centered on the receptive field; 440 nm: 10.9 log quanta·s^{-1}·deg^{-2}; 540 nm: 9.8 log quanta·s^{-1}·deg^{-2}; 640 nm: 10.6 log quanta·s^{-1}·deg^{-2}. Adapting background 10° arc; W: white light of 450 troland (td); B: 480-nm light of 8.6 log quanta·s^{-1}·deg^{-2}; R: 660-nm light of 8.6 log quanta·s^{-1}·deg^{-2};Y: 580-nm light of 7.6 log quanta·s^{-1}·deg^{-2}; M: 440-nm and 640-nm lights of 8.1 and 8.9 log quanta·s^{-1}·deg^{-2}. Pulse-density tracings in this and other figures represent the average of 30 responses; thin lines below each tracing represent 0 impulses/s, whereas thick lines represent the on-phase of the incremental stimulus. Calibrations: 30 impulses/s, 150 ms. Solid arrows point to off-responses.

circles) on a white background (W). The changes in the shape of the test action spectra on 480-nm (B) and 640-nm (R) backgrounds indicate concurrent input from red and green cones to the cell. In addition, an intense 580-nm background (Y) also re-

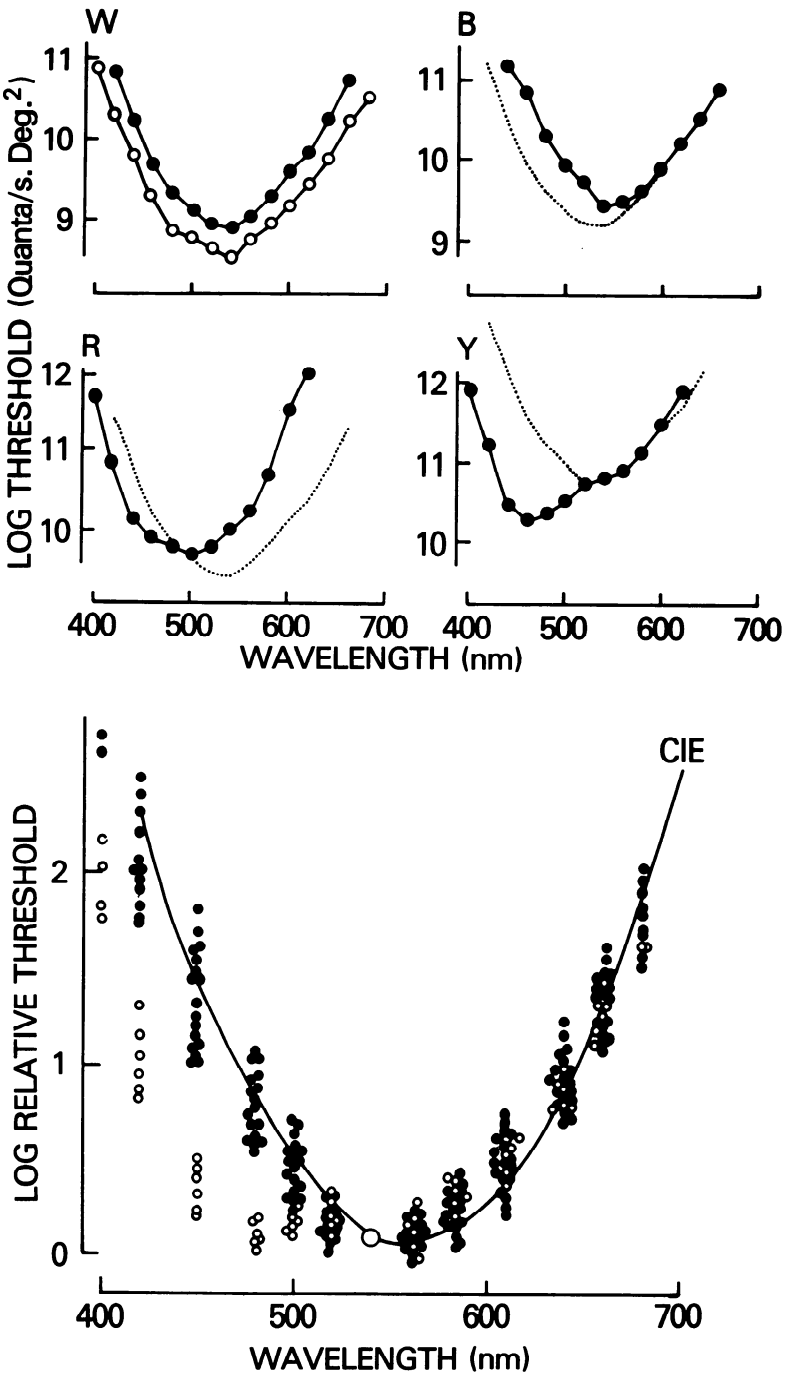

FIG. 2. *Top*: action spectra of a type III cell using a 0.2° (open circles) and a 0.4° spot (solid circles). Adapting background of 10°; W: white light of 450 td; B: 480-nm light of 8.6 log quanta·s^{-1}·deg^{-2}; R: 640-nm light of 8.6 log quanta·s^{-1}·deg^{-2}; Y: 580-nm light of 10.1 log quanta·s^{-1}·deg^{-2}. The dotted curves in B, R, and Y represent the action spectrum of W (solid circles). *Bottom*: superimposed test action spectra of 25 type III cells, obtained with 0.4–0.5° spots on a 580-nm background of 6.9 log quanta·s^{-1}·deg^{-2} (10°). The spectra have been normalized at 540 nm; the continuous line represents the C.I.E. photopic luminosity function. Open circles indicate those cells whose test sensitivity was broader than that of other cells at the short-wavelength band.

vealed a relative increase in wave-length sensitivity peaking at about 450–460 nm. The bottom part of Fig. 2 shows superimposed test spectral sensitivities of 25 type III cells which failed to show a Purkinje shift after 30 min of dark adaptation and presumably lacked significant input from rods; these spectra were obtained in the presence of a relatively weak yellow background and have been normalized at 540 nm. Whereas most cells had spectral sensitivities approaching the spectal distribution of the C.I.E. curve (solid line), six neurons had a broader sensitivity at the short wavelengths (open circles), suggesting the contribution of blue-cone signals to cell responses.

There were noteworthy differences between the polarity of center responses of these three cell types. All type IV cells were on-center, whereas about 68% of type III cells were on-center and 32% off-center; type I cells having green- or red-center were on-center in about 60% of the cases. There was a marked asymmetry in response polarity in cells in which blue-cone signals were opposed by concurrent signals from green and red cones (10): whereas almost 90% of blue-center cells were on-center, the relative incidence of blue-surround cells was similar to that of other type I varieties (e.g., about 40%). These differences have been confirmed on the basis of a much larger cell sample (unpublished observations).

X and Y identification

The summation of incoming cone signals to the cells was examined with a null test consisting of a rectangular bipartite field in which the contrast between the halves was reversed in antiphase using sine- or square-wave modulation (see METHODS). Since this stimulus was not a periodic one, e.g., sinusoidal grating, the mean illumination over the receptive field of a cell only remained constant during contrast reversal when the boundary between the hemifields was located at the point of receptive-field lateral symmetry, typically the field middle. This location was routinely used to examine the degree of linearity of spatial summation. The spatial summation of the cells was considered to be linear when a middle position could be found in which contrast reversal did not elicit a significant change in cell firing, i.e., a null position. This is shown in Fig. 3*A* using square-wave modulation of contrast reversal. Summation was considered to be nonlinear when a null could not be found and, in these cases, contrast reversal at the receptive-field middle always produced a doubling of the frequency of the responses, i.e., a second harmonic. This is shown in Fig. 3*B*.

The spatial summation of 232 cells of all three types was examined with this null test and the results indicated that whereas type I cells had a linear spatial summation, type III and IV cells had a nonlinear spatial summation.

Figure 4 responses of an off-center type I cell, green-center, red-surround, to sine-wave modulation of contrast reversal using a large null test. The top three pulse-density tracings of *A* and *B*, respectively, show center and surround responses elicited at different positions of the hemifields boundary using 480-nm (*A*) and 640-nm light (*B*) on a white background. The responses were the mirror image of one another and showed a null at the middle of the receptive field (second tracing), indicating that—for each opponent mechanism—a decrease of the illumination over one-half of the spatial region nullified the effects caused by the simultaneous increase of illumination over the remaining half of the mechanism in question. Responses in antiphase were elicited at symmetrically adjacent locations 0.04° apart from the middle of the receptive field (first and third tracings). Chromatic adaptation of the center or of the surround did not change the type of summation of the remaining mechanism, which still showed the same null position at the field middle (fourth tracing), indicating that the independent spatial summation of the center and surround mechanisms was linear and that both mechanisms shared the same null position. The bottom pulse-density tracings of Fig. 4 are control responses to the flashing of each half of the test stimulus when the boundary was located at the null position. It can be seen that responses elicited with either half were nearly identical to one another, indicating lateral symmetry.

The concurrent summation of the center and surround mechanism of the cells was examined with white-light tests, which also

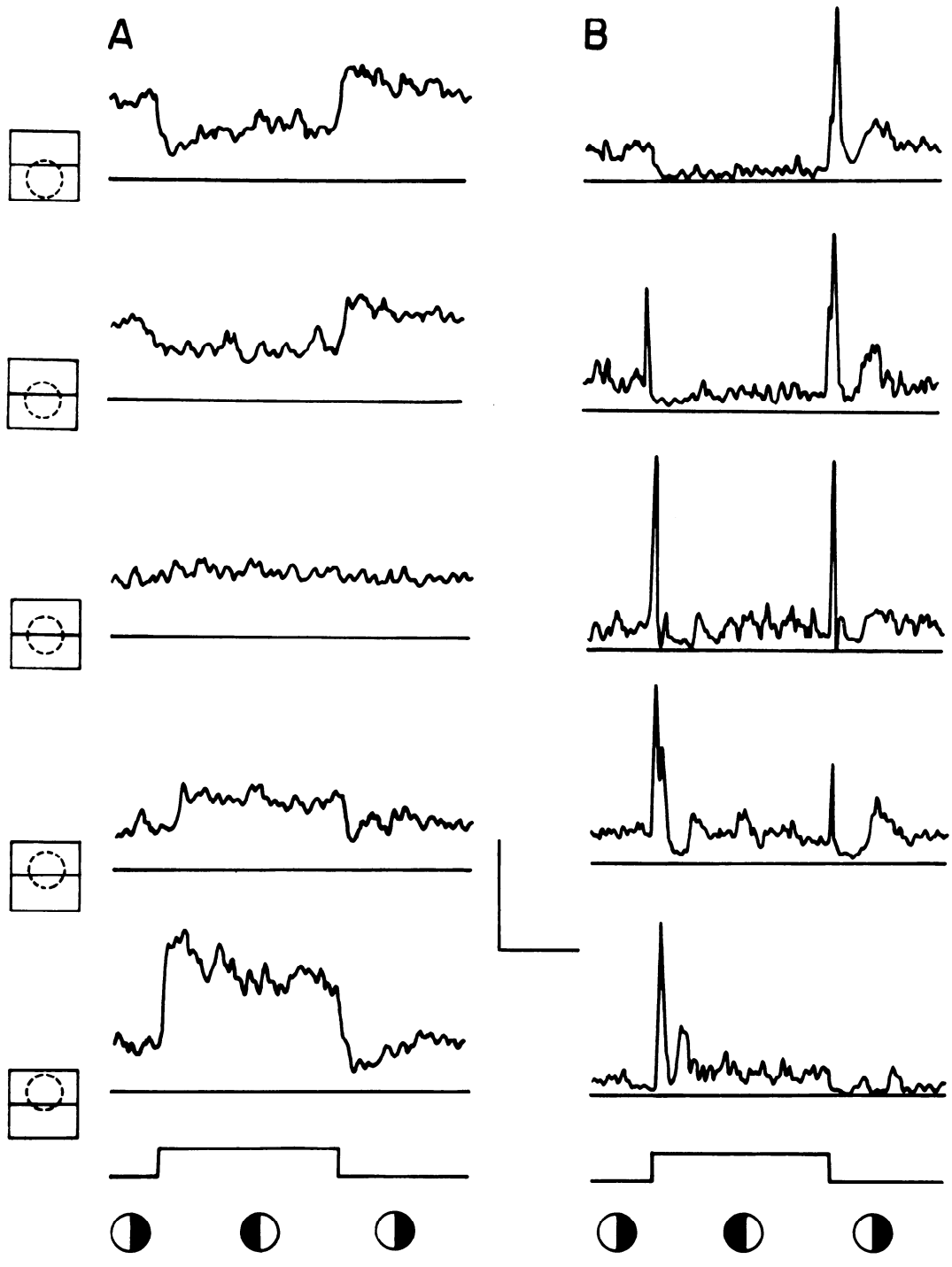

FIG. 3. Pulse-density tracings of responses of two ganglion cells to the square-wave reversal of contrast between halves of a bipartite field. Responses were elicited with hemifields boundary located at different positions across the receptive fields of cells. *A*: cell with linear spatial summation, as indicated by the null position found at the middle of the field (third tracing); *B*: cells with nonlinear spatial summation, as indicated by the presence of a doubling of response frequency when the boundary was located at the middle of the field (third tracing). The position of this boundary and the contrast between halves of the null test are, respectively, indicated at the left-hand side and at the bottom of tracings. Calibrations: 30 impulses/s, 230 ms.

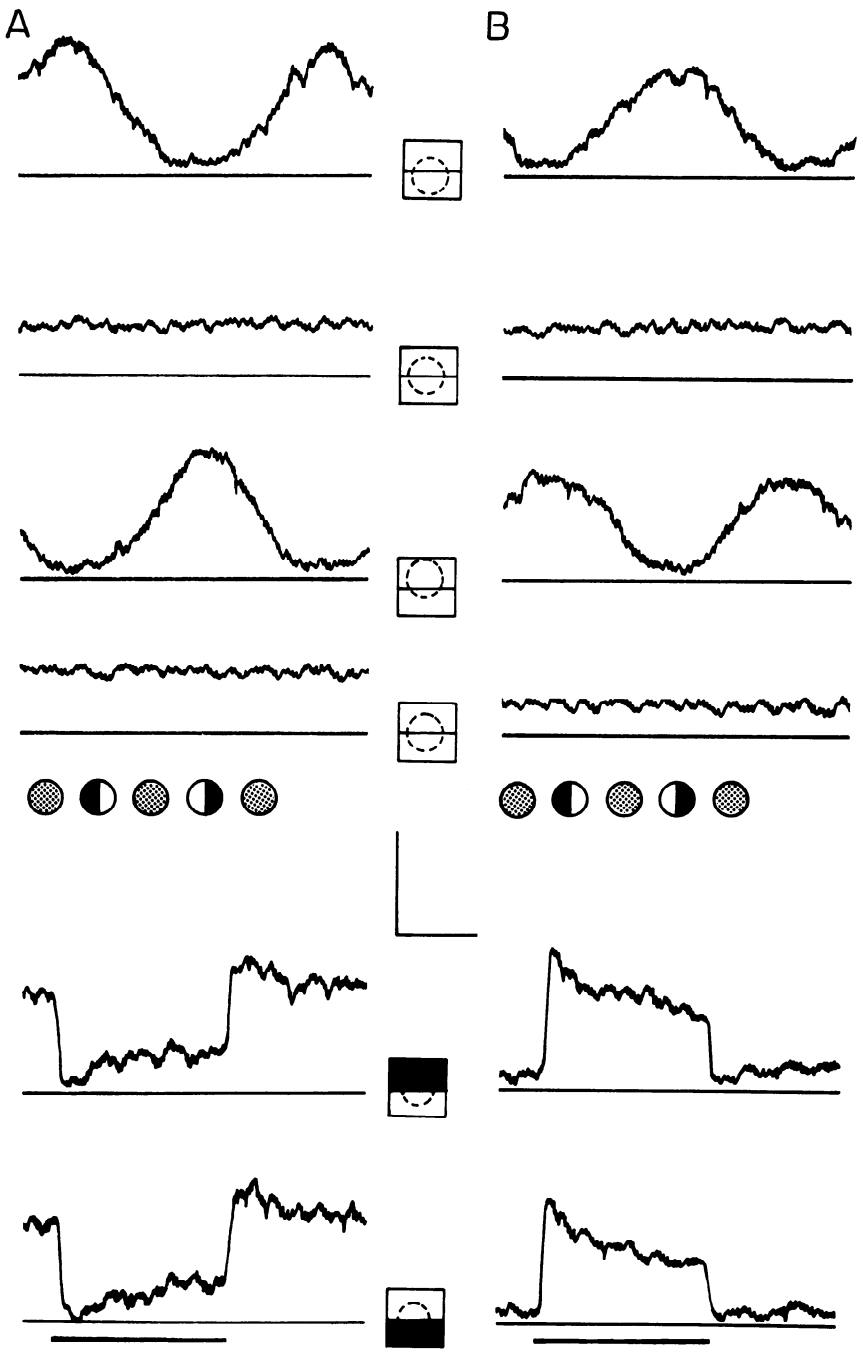

FIG. 4. Pulse-density tracings of center (*A*) and surround (*B*) responses of a type I cell having a green-off center, red-on surround elicited, respectively, with 480-nm and 640-nm lights on neutral and colored backgrounds. Top: responses to sinusoidal modulation of contrast of the null test on a white background (top three tracings) and on 640-nm (fourth tracing in *A*) and 480-nm backgrounds (fourth tracing in *B*) which were intense enough to adapt the opponent responses. Both responses showed a null position which was not modified by the chromatic adaptation of the opponent responses (compare second and fourth tracings). Bipartite field of 8° on the side, sinusoidal moduiation of 1.5 Hz; symbols at the bottom of tracings schematically represent changes of contrast between test hemifields. Bottom: responses to the flashing of each half of the test pattern when the boundary between hemifields was located at the middle of the receptive field (second tracing in *A* and *B*, top). Calibrations: 30 impulses/s, 350 ms.

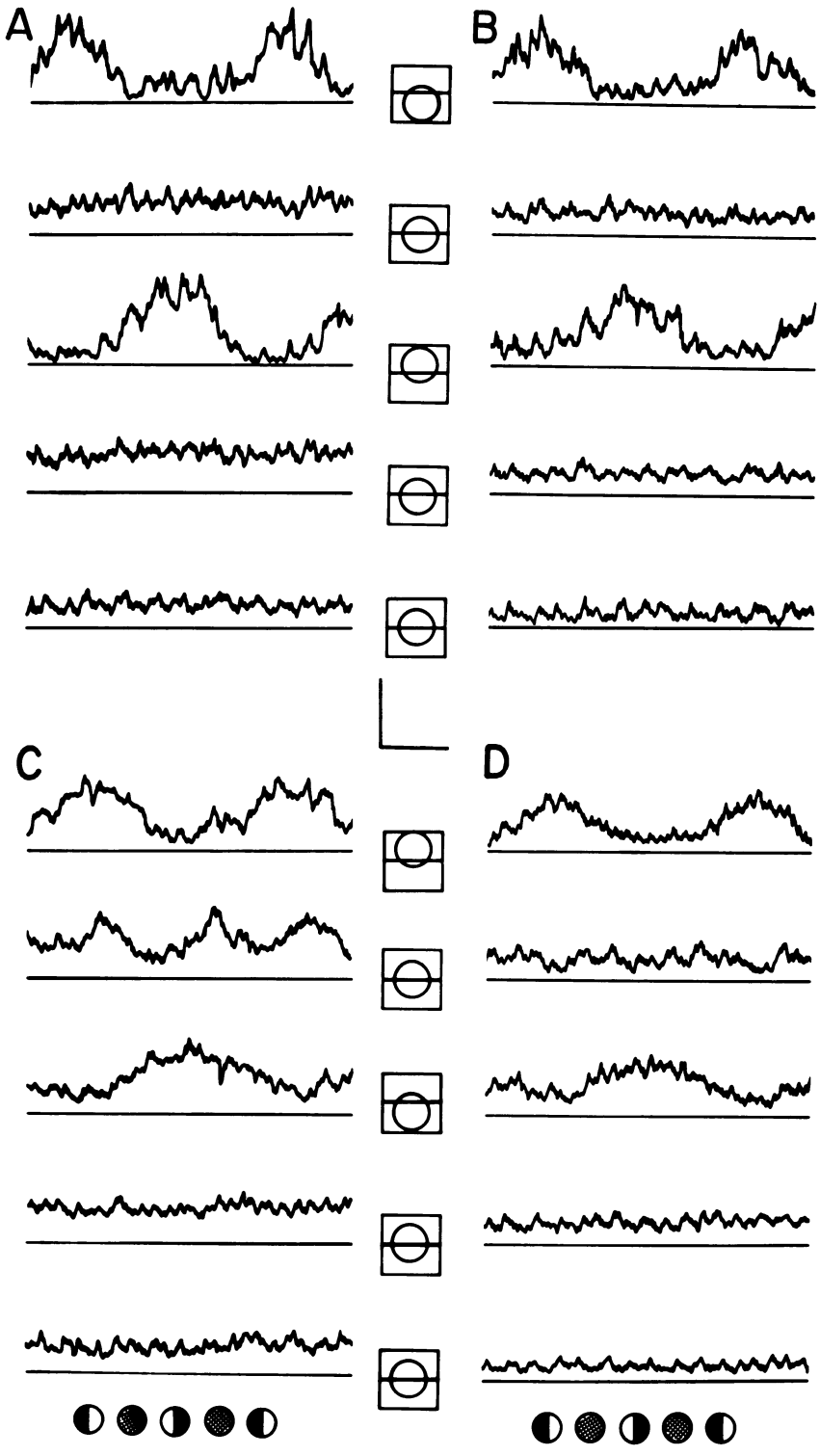

allowed the comparison of the summation of nonopponent and opponent-color cells. Figure 5*A* and *B* shows responses of the same type I cell using large and small null tests. The top three tracings again show responses at three different positions of the hemifield boundary in the presence of a white background; the concurrent summation was linear since a null position was found at the field middle (second tracing). This null position was maintained with a background adapting the surround (fourth tracing) and center responses (fifth tracing), as could be expected from the results shown in Fig. 4. This behavior was found in most type I cells (95%, 147/155), including all neurons having a "concealed" surround antagonism. The remaining 5%, however, showed a nonlinear summation to large null tests of white light, but a linear summation to small tests of white light and to any null test of monochromatic light favoring either center or surround responses. Differently from the other cells, however, monochromatic null tests indicated that the null positions for the center and the surround mechanisms of these type I cells were not coincident. Figure 5*C* and *D* shows responses of one such cell to large and small null tests of white light. An obvious doubling of the response modulation was elicited at the middle of the field with the large test; this doubling disappeared on backgrounds adapting either opponent mechanism (fourth and fifth tracings), although the null position for the spatial summation in conditions of center adaptation was laterally displaced from the middle of the field. The summation of this cell also became linear simply by reducing the size of the null test to the dimensions of the receptive-field center, as shown in *D*.

These type I cells having such a "mixed" type of spatial summation were often located away from the foveal region. They had a comparatively strong surround antagonism of center responses (e.g., diffuse white lights elicited predominantly surround responses) and showed conspicuous off-responses similar to those of type III and IV cells (7). Area threshold measurements obtained in conditions of selective chromatic adaptation of the cone type overtly mediating surround responses showed that there was a marked increase in the threshold for stimuli larger than the receptive-field center. This resembled the behavior of nonopponent-color cells, suggesting the presence of mixed cone inputs to the opponent regions; similar results have been obtained in other studies (e.g., Fig. 12 of Ref. 17).

The majority of type III cells had an obviously nonlinear summation to monochromatic and white-light null tests, i.e., a doubling of response frequency instead of a null response at the middle of the receptive field. Only two cells showing overt surround antagonism and the few cells having a concealed surround antagonism (see above) showed an apparent linear summation. This distinction, however, was dependent on the center-surround sensitivity balance. Figure 6 shows responses of two on-center type III cells, one with overt (*A*) and the other with concealed (*B*) spatial opponency. The top three tracings show responses elicited at different locations of the receptive field; whereas the cell with overt opponency showed a second harmonic at the field middle, the cell with concealed opponency showed a null position (second tracing). The fourth and fifth tracings of both figures, respectively, show the effects of light adaptation of the center (steady small spot) and of the surround (steady large annulus). Although light adaptation of the center did not alter the nonlinear summation of the

FIG. 5. Spatial summation of type I cells to white-light null tests. *A*: white-light test of 8° on the side, with a mean illuminance of ca. 130 td; *B*: responses of the same cell to a white-light test of 0.08° on the side with a mean illuminance of ca. 300 td. The top three tracings of each figure show responses elicited with three different positions of the bipartite field across the receptive-field center in the presence of a superimposed background of ca. 100 td; the second tracing shows the existence of a null position for both test configurations. The fourth and fifth tracings, respectively, show responses obtained at the same null position in the presence of chromatic adaptation of the surround (640-nm light of 9.3 log quanta$\cdot s^{-1}\cdot deg^{-2}$) and the center (480-nm light of 10.1 log quanta$\cdot s^{-1}\cdot deg^{-2}$). Center size of 0.09° at 1/*e* of the peak sensitivity. *C* and *D*: responses of another type I cell having the same chromatic organization that showed linear summation to monochromatic tests of center or surround summation. This neuron had a nonlinear summation to large null tests of white light (*C*) but linear summation to small tests (*D*). Other parameters as in *A* and *B*. Center size of 0.075° at 1/*e* of the peak sensitivity. Modulation depth 0.6 log unit, mean illuminance 1 log unit above cell threshold. Calibrations: 30 impulses/s, 300 ms. Symbols at the bottom of tracings schematically represent changes of contrast between test hemifields. Both neurons were encountered in the same parafoveal penetration.

overt spatially opponent cell, it led to the doubling of the frequency of responses now elicited at the middle of the field of the cell having concealed spatial opponency. The reverse effects were produced by light adaptation of the surround, both cells then showing a null position at the field middle. These and other results obtained from 61 type III cells suggested that their nonlinear summation to both small and large null tests

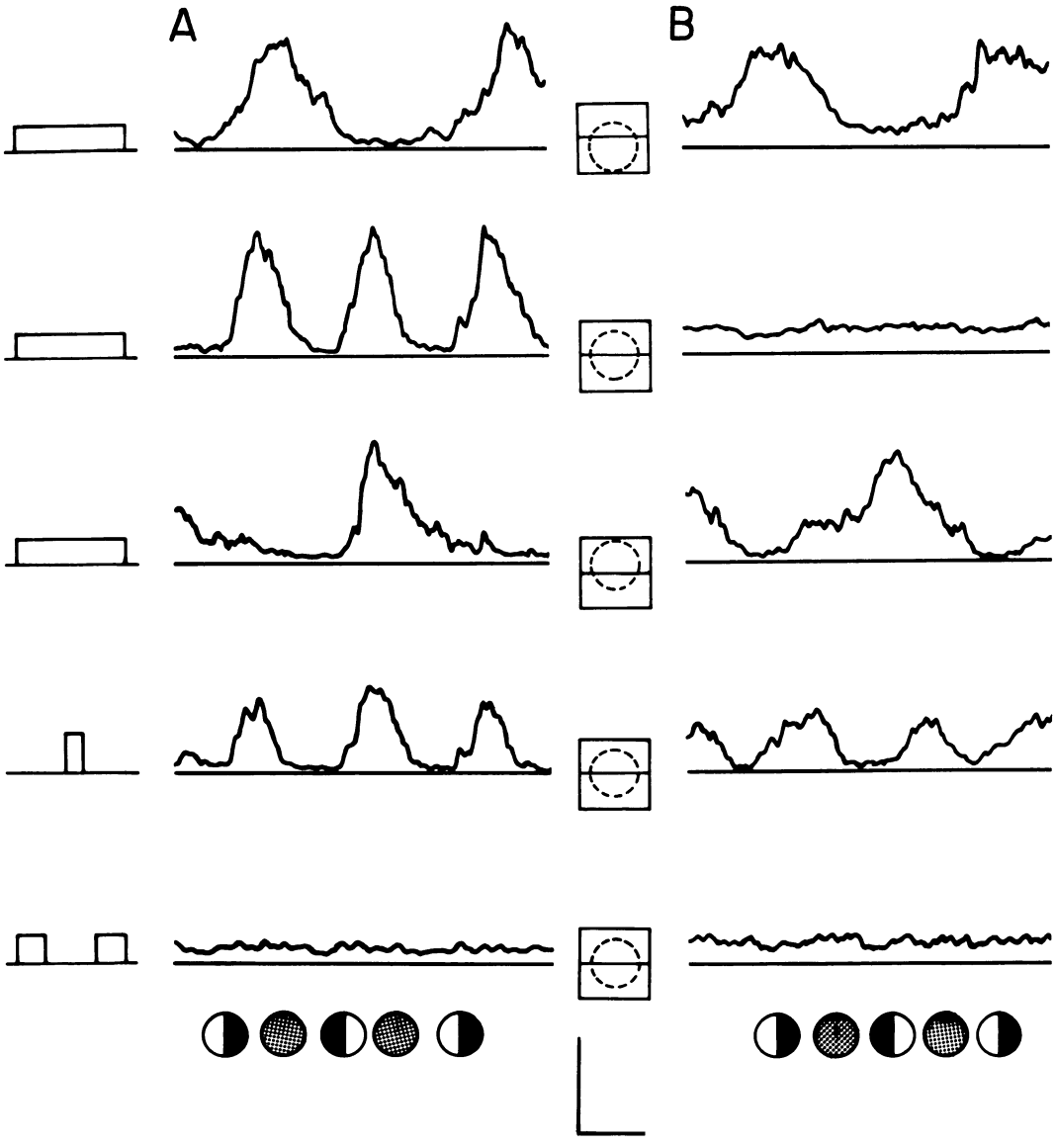

FIG. 6. Responses of type III cells to a white-light null test in different conditions of light-adaptation; one neuron had overt spatial opponency (*A*), whereas in the other, (*B*) opponent surround responses were concealed in the absence of light adaptation of the center. The top three tracings were obtained with different positions of the null test in the presence of a diffuse white background of 200 td in *A* (center size of 0.15° at 1/*e* of peak sensitivity) and 140 td in *B* (center size of 0.21 at 1/*e* of peak sensitivity). The bottom two tracings were obtained in the respective presence of a steady spot of center size (500 td) and a steady annulus with an inner diameter of 1° (400 td). Symbols at the bottom of tracings depict changes in the contrast between test hemifields. Both neurons showed linear summation in conditions of light adaptation of the surround and nonlinear summation in conditions of light adaptation of the center. Calibrations: 30 impulses/s, 250 ms. Symbols at the bottom of tracings depict changes in contrast between the test hemifields.

was dependent on the surround mechanism and that the summation of the center mechanism in conditions of relative isolation was linear.

This interpretation was tested in type IV cells by taking advantage of the spectral opponency of the cells. Figure 7 shows responses of a type IV cell to large (*A*) and small (*B*) null tests; the center of this cell received input from red and green cones, whereas its surround received input from red cones alone. The top three tracings show responses elicited with white-light null tests on a white background; small and large tests elicited a second harmonic at the field middle (second tracing), indicating nonlinear summation, and the same result was obtained using a 480-nm test on the same background (fourth tracing). A null position, however, was found at the middle of the field

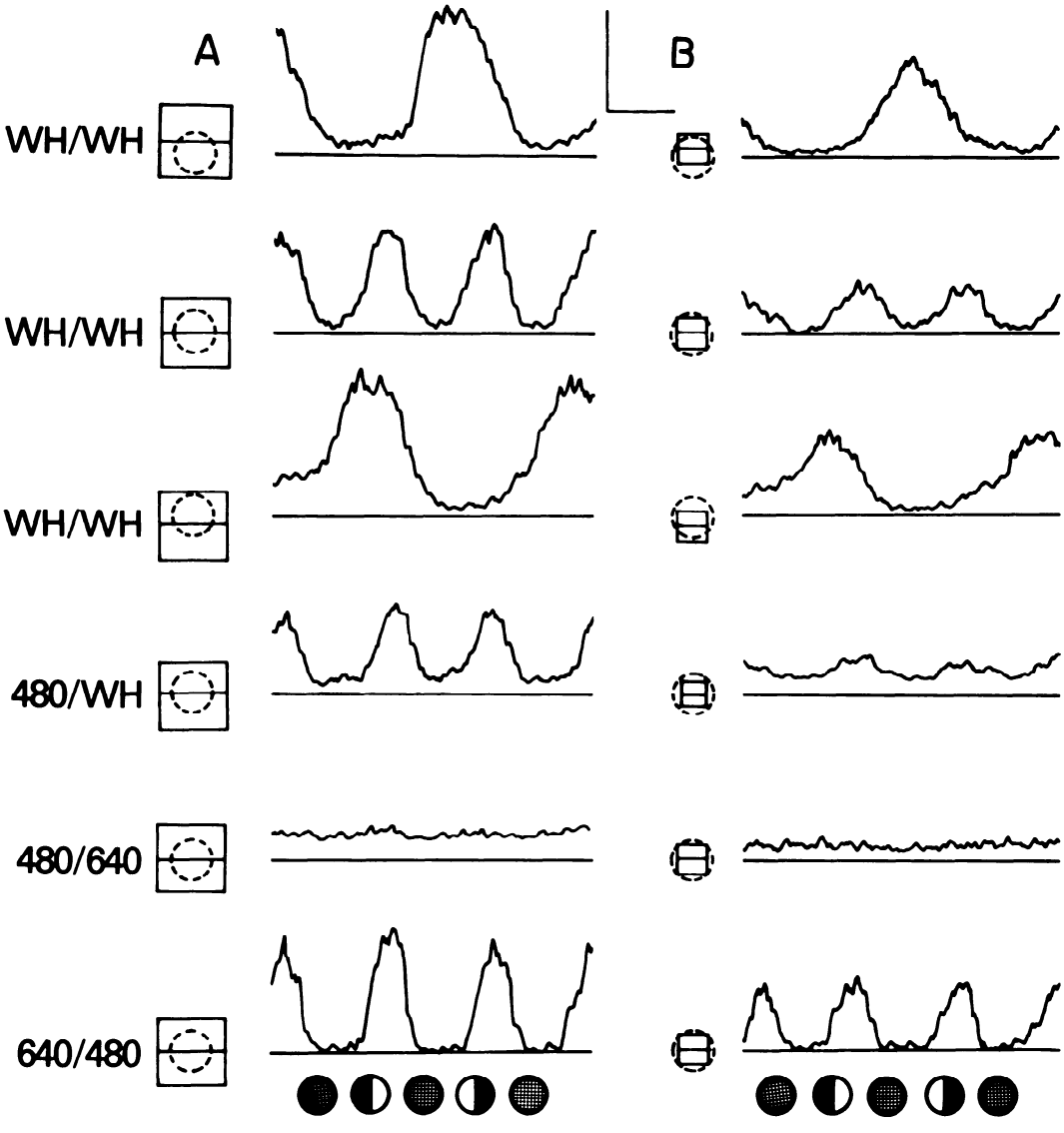

FIG. 7. Responses of a type IV cell to large (*A*) and small (*B*) null tests and backgrounds of different spectral composition. The neuron showed nonlinear summation to null tests in conditions of neutral adaptation or chromatic adaptation of the noncommon cone input to the center, while it showed a linear summation in conditions of chromatic adaptation of the cone input to both opponent regions. Calibrations: 30 impulses/s, 250 ms. Symbols at the bottom of tracings depict changes in contrast between test hemifields.

using the 480-nm test in the presence of a 640-nm background (fifth tracing), whereas a doubling of response modulation was again obtained by reversing the wavelength of the test and the background (sixth tracing). Whereas the 640-nm background adapted the red-cone signals to both opponent regions, the 480-nm background adapted the green-cone signals to the center; these results thus provide evidence that the nonlinear process was located within the surround mechanism. The nonlinear behavior of type III and IV cells to white-light tests was maintained when using small tests whose dimensions were smaller than that of the receptive-field center, suggesting that the surround mechanism of these cells had a comparatively high sensitivity toward the middle of the receptive field.

Drifting sinusoidal gratings

Ancillary experiments using unidirectionally drifting sinusoidal gratings supported the identification of type I cells as X-cells, permitting its extension to those few neurons having a mixed type of summation to monochromatic and white-light tests, and the identification of type III and IV cells as Y-cells (16).

Figure 8 shows center (*A*) and surround (*B*) responses to 480- and 640-nm gratings on a white background, which were elicited from an on-center type I cell having a green-center, red-surround organization. It can be observed that there was a periodic modulation of cell firing at the drift frequency, essentially having the same mean value at the various spatial frequencies and which was similar to that of the maintained discharge of the cell to a uniform field (UF) having the same wavelength and mean luminance as the gratings. Figure 8*C* and *D* shows responses to white-light gratings elicited from type I cells respectively having linear and mixed summation to white-light null tests. Although the responses differed in their degree of distortion at the low spatial frequencies, both neurons showed a periodic modulation of their discharges essentially having the same mean value for different spatial frequencies.

Figure 9 shows responses of a type IV cell to white-light gratings on various adapting backgrounds. Responses in *A* were obtained with gratings preceded by a uniform field having the same mean luminance (initial segment of the tracings) and the stimulation was restricted to an area of 10° centered on the receptive field in the presence of a diffuse white background. Low spatial frequencies produced a doubling of response frequency, i.e., the cell was excited by the dark and light areas of the gratings. This behavior disappeared at higher spatial frequencies, which produced a modulation of cell firing at the drift frequency whose mean value was higher than that to the uniform field preceding the grating (solid arrowhead). Gratings with the highest available spatial frequency often generated an unmodulated cell activity whose mean value also was higher than that to the uniform field (bottom tracing), although the neurons typically responded to the leading edge of the gratings. Chromatic adaption of the cone type mediating surround and, partly, center responses, i.e., red cones in this cell, attenuated waveform distortion at the low spatial frequencies and abolished the unmodulated activity elicited by the high spatial frequencies. This is shown in Fig. 9*B* using a 660-nm background. In addition, surround adaptation also tended to produce modulation of cell firing with a mean value similar to that to the uniform field (UF). Reduction of the area being stimulated by the gratings to the dimensions of the receptive-field center did not appreciably modify the behavior observed with large patterns, although it increased the range of both low and high spatial frequencies to which the cell responded in a manner similar to that observed during conditions of surround adaptation. Figure 9*C* shows that such small patterns, however, still elicited waveform distortion at the low spatial frequencies and unmodulated activity at the high frequencies.

The results of these experiments indicated that whereas type I cells showed a periodic modulation of their discharge having the same value for different spatial frequencies, types III and IV cells showed a large increase in the mean value of their discharges which could be abolished by illuminating conditions depressing surround sensitivity. These properties, coupled with the results of null test experiments, indicate that the spatial summation of these two groups of neurons, respectively, resemble that of X- and Y-cells of the cat retina (16).

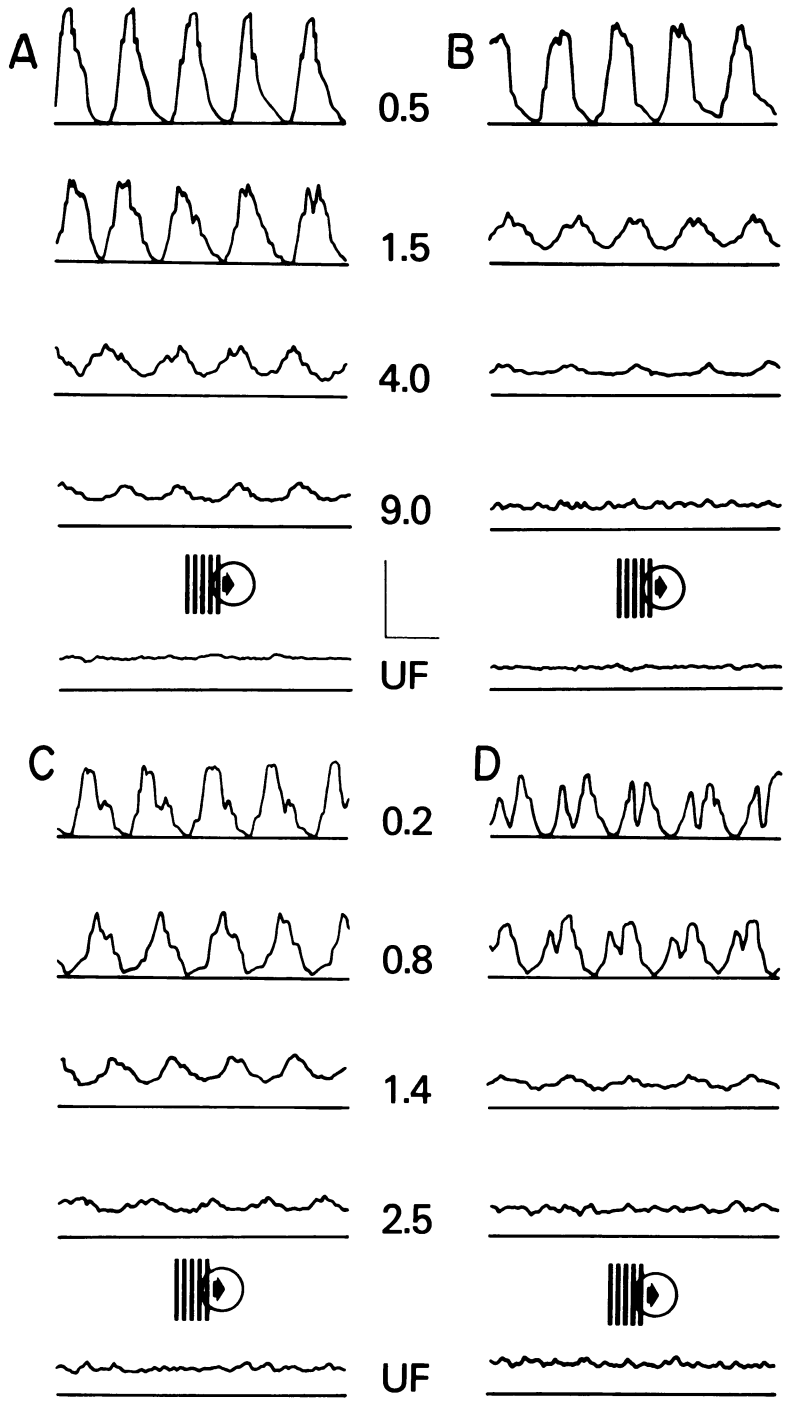

FIG. 8. Responses of type I cells to monochromatic and white-light sinusoidal gratings drifting in one direction of motion. *A*: center responses to 480-nm gratings (mean energy of 8.2 log quanta·s^{-1}·deg^{-2}) on a white background of 200 td. *B*: surround responses of the same cell to 660-nm gratings (mean energy of 7.5 log quanta·s^{-1}·deg^{-2}) on a white background of 250 td. *C*: responses of the same cell to a white-light grating (mean illuminance of 400 td) on a white background of 200 td. *D*: responses of a different type I cell to white-light gratings (mean illuminance 350 td) on a white background of ca. 300 td. Numbers represent cycles per degree, while UF shows responses to a uniform field of the same mean luminance and wavelength as those of the gratings. Drift frequency of 5 Hz; calibrations: 30 impulses/s, 180 ms.

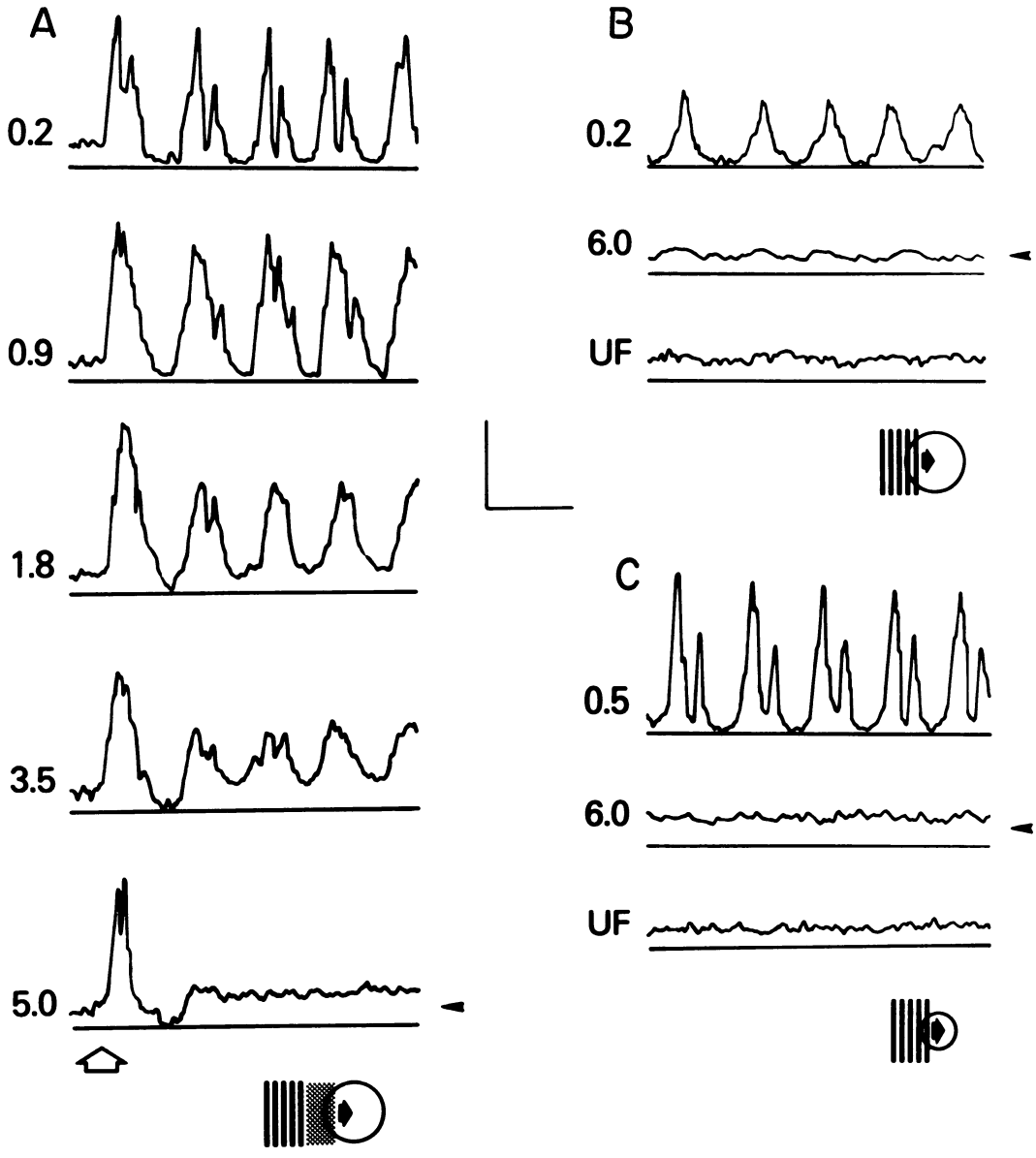

FIG. 9. Responses of a type IV cell to drifting sinusoidal gratings. *A*: white-light gratings (mean illuminance 500 td) on a white background of 250 td. These gratings were preceded by a uniform field having the same mean luminance as the patterns; open arrow points to responses to the leading edge of the gratings, whereas solid arrowhead points to the mean level of background cell activity during the presentation of the uniform field. *B*: same gratings in the presence of a colored background depressing the sensitivity of the common cone mechanism mediating both center and surround responses (660-nm light of 9.7 log quanta $\cdot s^{-1} \cdot deg^{-2}$). *C*: white-light gratings on a white background similar to those of *A*; patterns were restricted to the central part of the receptive field by interposing an annular mask of 0.15° in inner diameter centered on the field. Solid arrowheads indicate the mean level of background cell activity produced by the presentation of a uniform field (UF) of the same spectral composition and mean illuminance as those of gratings. Numbers on the left-hand side of tracings indicate the spatial frequency of gratings in cycles per degree. Drift frequency of 5 Hz. Calibrations: 30 impulses/s, 250 ms. Gratings in *B* and *C* were not preceded by a uniform field.

The following sections describe functional properties of these two groups of macaque ganglion cells.

Conduction latencies

Figure 10*A* shows the distribution of conduction latencies of antidromic responses elicited by electrical stimulation of the corresponding optic tract in 185 cells of both groups, which were located within the temporal 15° of the retina close to the horizontal meridian. All three cell types had distributions with considerable overlap, although type I (X) cells had longer latencies (open blocks) than type III and IV (Y) cells (solid blocks). The mean value of the latency of the former cells was 9.44 ± 0.24 (SE) ms (n = 102), while that of the latter cells was 5.65 ± 0.81 (SE) ms (n = 83). Among type I cells, however, blue-center neurons had shorter latencies than other type I varieties (unpublished observations).

Central projections

Figure 10*B* shows mass responses recorded with the optic tract (OT), lateral geniculate body (LGB), and superior colliculus (SC) stimulating electrodes; these responses were elicited with a diffuse light flash starting at the beginning of each one

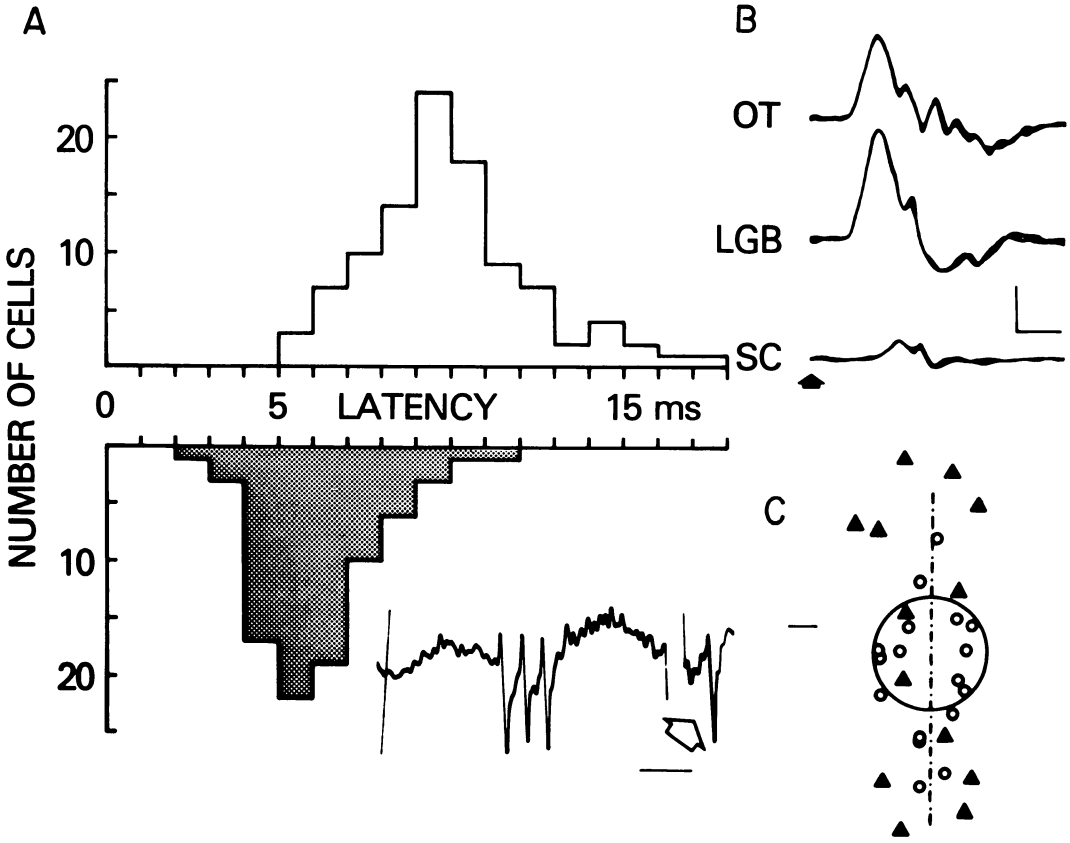

FIG. 10. *A*: distribution of the conduction latencies of 102 type I cells (open blocks) and 83 type III and IV cells (dotted blocks); antidromic responses elicited by electrical stimulation (1.5× current threshold) of the ipsilateral optic tract. Record at the bottom shows three orthodromic responses elicited in conditions of diffuse stimulation of the receptive field with white light and an antidromic response (open arrow) elicited from the optic tract in a type III cell; calibration bar: 5 ms. *B*: mass-response recordings obtained with electrodes located in the optic tract (OT), lateral geniculate body (LGB), and superior colliculus (SC) during stimulation with a brief flash of diffuse light (arrow). Three responses have been superimposed in each record; calibrations: 0.4 mV, 20 ms. *C*: retinal location of the receptive field of nasally located cells that projected to the ipsilateral optic tract and of temporally located cells that projected to the contralateral optic tract in two animals. The interrupted line indicates the vertical retinal meridian, while the circle represents the foveal boundaries. Open circles indicate crossed type I cells, solid triangles indicate crossed type III cells. calibration bar: 1° arc.

of the three superimposed traces of the different responses (solid arrow). Electrical stimulation with the geniculate electrode pairs elicited antidromic responses in about 65% of type I cells and in about 55% of type III and IV cells; the more posterior and superficial electrode tended to favor the activation of the former neurons. Electrical stimulation with the collicular electrode pairs failed to elicit antidromic responses of type I and type IV cells. A fraction of type III cells (about 11%), located within 1 and 15° of retinal eccentricity, were antidromically driven from the superior colliculus. Many of these cells were encountered close to opponent-color cells which could not be driven by collicular stimulation; none of the type III cells having collicular projections appeared to receive input from blue cones.

Figure 10*C* shows the retinal location of the receptive field of cells "crossing" the vertical meridian of the left eye of two animals, i.e., nasally located cells which projected to the left optic tract and temporally located cells which projected to the right optic tract. Most of the extrafoveal overlap of type I cells (open circles) was confined to a median strip 1° wide, although crossed extrafoveal type I cells were occasionally found in median strip 2° wide. Foveal overlap across the vertical meridian was more frequently observed in cells of this type, occupying an annular region of about 3° in outer diameter. Ipsilaterally and contralaterally projecting type III cells overlapped across the vertical meridan by as far as 1.5°, especially in the extrafoveal region (solid triangles); very few examples of crossed type III cells were found in the foveal region.

Retinal distribution

Table 1 illustrates the retinal distribution of the 377 ganglion cells of the sample. Type I cells were found at all examined eccentricities with a comparable high incidence. They had a relative predominance over other cell types in the central 10° of the retina (see DISCUSSION) and appeared to peak at 0.5–2° of eccentricity. As previously observed (9), green-center neurons predominated over red-center neurons between 0.5 and 5°, whereas the reverse situation was observed beyond 5–10° of eccentricity. In contrast, blue-center cells appeared to peak between 2 and 5° and had a comparatively low incidence below 1° of eccentricity. Type III cells had a comparatively high incidence toward the more peripheral region of the extrafoveal retina and were less commonly encountered below 2°; type IV cells were frequently encountered between 2 and 10° of eccentricity, but rarely at the fovea.

Response time course

The responses of all cell types to an incremental stimulus consisted of excitatory or inhibitory changes of cell firing in relation to the level of maintained activity. Previous retinal studies (17, 23) have reported that ganglion cells can be classed according to the degree of transience of the responses to "small" stimuli centered on the receptive field. Based on such criteria, opponent-color and nonopponent-color cells, respectively, have been tagged "tonic" and "phasic" cells (17). Moreover, response time course has been used as one of the criteria to distinguish between X-like and Y-like cells (14).

TABLE 1. *Retinal distribution of 377 concentrically organized ganglion cells*

Retinal Eccentricity, deg	Type I			Type III	Type IV	Total
	Green center	Red center	Blue center			
0–0.5	14 (50)	10 (36)	1 (4)	2 (7)	1 (4)	28
0.5–1	12 (36)	11 (33)	3 (9)	4 (12)	3 (9)	33
1–2	15 (29)	14 (27)	5 (10)	10 (19)	8 (15)	52
2–5	13 (21)	12 (20)	7 (12)	18 (30)	11 (18)	61
5–10	16 (22)	19 (26)	4 (5)	28 (33)	6 (8)	73
10–20	21 (16)	30 (23)	8 (6)	66 (51)	5 (4)	130
Total	91	96	28	128	34	

Green-center and red-center include red-green-center, blue-surround cells grouped according to the predominant cone input to the center. Values in parentheses represent percent frequency relative to the eccentricity yield at the retinal region.

Since the discharge pattern of ganglion cells is dependent on the center-surround balance of antagonistic signals (20), the time course of the responses of cell types I, III and IV was examined using equivalent conditions of stimulation. It is known (2) that variations in the background illuminance predominantly affect the sensitivity of surround responses. The use of the same adapting background, however, does not insure a similar degree of light adaptation for all of the cells if these have receptive fields of different dimensions; more uniform conditions of light adaptation can be obtained by adjusting the intensity of the background so that the product (background intensity × receptive-field size) is similar for all of the cells. If one assumes a monotonic relation between the size of the receptive-field center and that of the surround, the more accessible product (background intensity × center size) may be used as an approximation. Figure 11*A* shows the distribution of the ratio of cell firing during the initial and final 100 ms of the stimulus (1 s) measured in 60 type I cells (open blocks), 50 type III cells (dotted blocks), and 28 type IV cells (solid blocks) during equivalent conditions of light adaptation with a neutral white background. The responses were elicited with a spot of white light (in order to compare opponent and nonopponent color responses) whose diameter was equal to the 1/*e* peak sensitivity diameter of the center and with an intensity of 1 log unit above threshold. Whereas the distribution of type IV cells was unimodal, those of type I and III cells were bimodal. The mode close to ratio unity was due to those neurons having surround responses too weak to be observed without light adaptation of center responses (see above), while the other mode at higher ratio values was due to cells with a more typical center-surround antagonism. Type III cells showed an incipient third mode at large ratio values that was due to a few foveal neurons having atypically powerful surround antagonism (see above). Although having different means, the distributions had marked overlap and extreme examples with the opposite degree of transience were found. Figure 11*B* illustrates the distribution of the ratio of initial and final cell firing to the same spots but in the presence of conditions depressing the sensitivity of the surround: colored backgrounds in type I and IV cells and a steady white-light annulus in type III cells. In these conditions, the distributions were laterally displaced toward ratio unity, became narrower, and had more overlap than the distributions observed in the absence of surround adaptation.

The results indicate that, although type I cells tended to have more sustained responses than those of type III and IV cells, degree of transience to a small spot centered on the receptive field represented tendencies rather than invariant center properties. Whereas a phasic/tonic or transient/sustained distinction may have some classificatory value and perhaps functional significance, the above-described measurements indicate that such distinction can depend on the center-surround balance, even in the case of small spots geometrically restricted to the center. With very few exceptions, variations of the intensity, spectral composition, and stimulus geometry (most of which did not appreciably affect the type of spatial summation) were found to transform phasic into tonic responses, and vice-versa.

DISCUSSION

Macaque ganglion cells can be classed as X- or Y-cells on the basis of tests similar to those originally used by Enroth-Cugell and Robson (16) to study cells in the cat retina. The results show that the degree of linearity of spatial summation of incoming (cone) signals to the neurons is related to the degree of cone specificity of the chromatic mechanisms mediating center and surround mechanisms (e.g., type I vs. type III and IV cells) and not to the presence or absence of opponent-color responses (e.g., type I and IV vs. type III cells), as it has been occasionally implied or suggested on the basis of classifications that have not always retained the criterion of linearity (1, 14, 19, 21, 23).

In addition to extending the X/Y distinction to the retina of a primate, the results show that there are appreciable differences in the retinal organization of macaque ganglion cells. The finding of a null position means that photoreceptor signals add linearly within the center and within the surround network of an X-cell, so that during

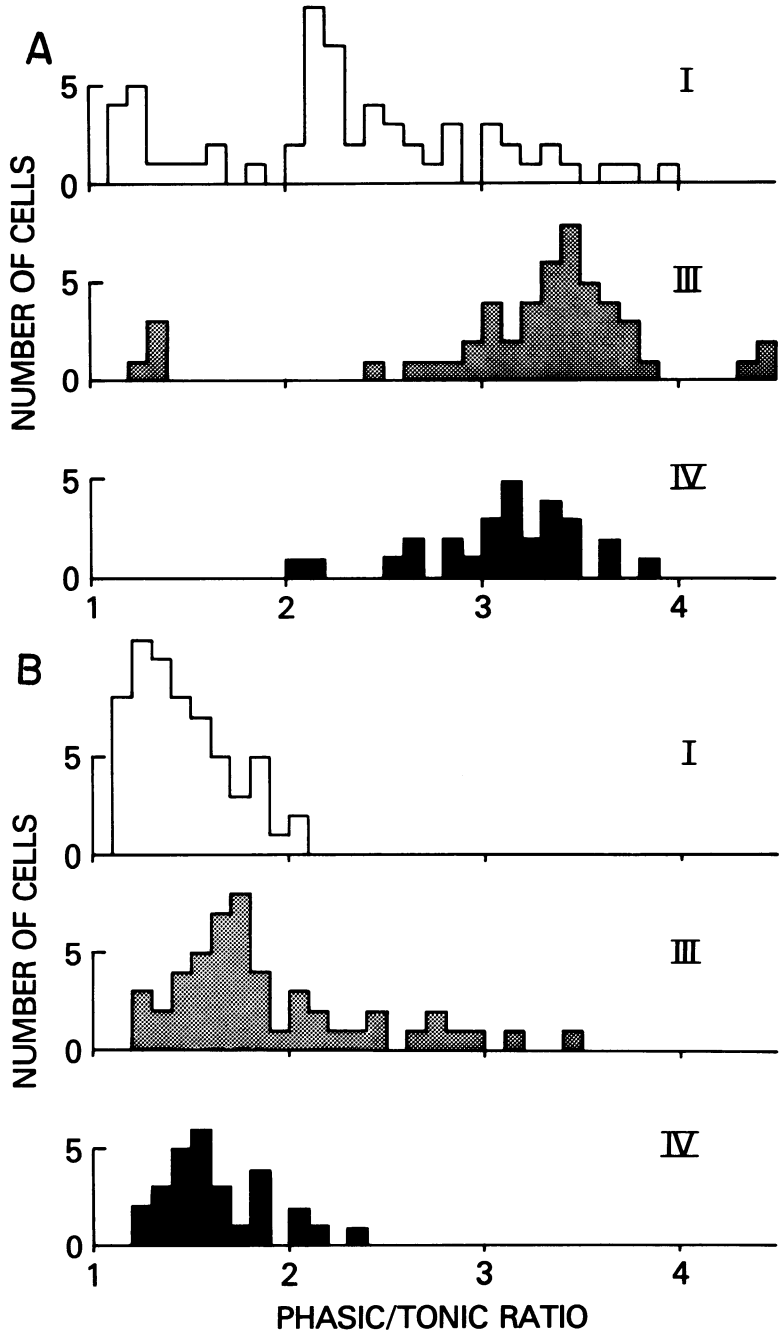

FIG. 11. Distribution of the ratio between cell firing during the initial and final 100 ms of the on-phase of the stimulus, measured in 60 type I, 50 type III, and 28 type IV cells, all of which were on-center. *A*: distribution in the presence of a white background presumably producing similar degrees of light adaptation in all cells (see text). *B*: distribution in the presence of adaptation of the surround mechanism (colored backgrounds in type I and IV cells, steady annulus of white light in type III cells). Data obtained from pulse-density tracings of responses to a spot having a diameter equal to the 1/*e* peak sensitivity diameter of the receptive-field center.

contrast reversal of the grating there is no net change in each one of these mechanisms and, consequently, there is no change in cell output. It is worth stressing that such null output is due to the cancellation of signals from one mechanism (e.g., center) by opposite signals from the same mechanism (e.g., center), and not due to the cancellation of center signals by opposite surround signals, as it has been recently suggested (1). This can be shown in opponent-color X-cells, which show a null position when either center or surround summation is examined in conditions of chromatic isolation, which also indicates that the presynaptic elements to the center and to the surround have an acceptable linear summation. Given the results of intracellular studies of the retina of other vertebrates (25), it is conceivable that the midget system (3, 22) is involved in the X-cell channel, in agreement with the suggestion that some type I cells (e.g., green- and red-center) may be midget ganglion cells (9). Whereas most type I cells can be classed as X-cells, a minority of these neurons fails to show a null position when the summation of both opponent mechanisms is concurrently examined, though these cells do show a null when the isolated summation of the center or of the surround is tested in conditions of chromatic adaptation of the opponent mechanism. Differently from true Y-cells, however, the nonlinear behavior of these type I cells to white-light null tests is dependent on the size of the test and they do not seem to show a Y-like behavior to drifting gratings. As it has been suggested for some X-cells of the cat retina (18), the behavior of these neurons may be due to a nonlinearity in the surround mechanism after its stage of spatial pooling. From this point of view it is likely that the neurons would show a null position for an alternating grating with fewer low spatial frequencies than a bipartite field.

The presence of a doubling of response frequency (e.g., second harmonic) instead of null responses from an isolated mechanism indicates that there is a nonlinear process prior to the combination of the signals from the opponent mechanisms to the cell (16). Types III and IV cells maintain their nonlinear behavior to null tests and drifting gratings, whether these patterns occupy the entire receptive field or are restricted to the central part of the field. This indicates that such behavior is mediated by a process having effective dimensions as small as or smaller than those of the center mechanism, especially in the case of cells showing unmodulated activity to gratings of high spatial frequency; cells of this group are thus unlikely to show a null position for a null test with fewer low spatial-frequency components than a bipartite field. The results also indicate that the spatial summation of the center mechanism of most Y-cells is acceptably linear in conditions of light adaptation of the surround mechanism, whereas that of the surround is nonlinear in conditions of light adaptation of the center; these observations suggest that the type III X-cells described by Dreher, Fukada, and Rodieck (14) may have been Y-cells with concealed spatial opponency rather than actual X-cells. Hence, in spite of the small effective dimensions and of the central location of the nonlinear process, these observations provide evidence that such a process influences the pooling of signals to the surround mechanism of Y-cells of macaques. The following paper (7) describes effects mediated by a mechanism with similar properties and that may be related to amacrine cell input to type IV cells. The inferences above described are consistent with those advanced for cat Y-cells (18).

Whereas the present results generally agree with those reported by Schiller and Malpeli (23), there is an apparent discrepancy between the retinal distribution of cell types of both samples. Based on axonal and cell-body recordings (the latter considered to generate fewer electrode sampling biases than the former; Ref. 23, p. 441), these authors concluded that their X-like (color opponent) and Y-like (broad band) cells had similar retinal distributions. This conclusion may be questioned. The cell-body sample of their Fig. 18 (bottom) shows that fewer cells of either group were encountered in the central 10° (ca. 30%) than between 10 and 20° (ca. 70%), indicating a sampling bias against centrally located neurons. If, in order to compensate for this bias, the distributions of the 127 X-like cells and of the 36 Y-like cells shown in this figure are replotted using percent frequencies of each region instead of raw cell numbers, one finds that whereas X-like cells represented ca. 90% between 1 and 10° and ca. 70% between 11 and 20°, Y-like cells,

respectively, represented ca. 10 and ca. 30% in these regions. Such distributions are in general agreement with those of the present and other studies (9). In the absence of more compelling evidence, it seems tenable that X and Y retinal distributions corrected for eccentricity yield are dissimilar.

X-cells tend to have more sustained responses, longer conduction latencies, and a more central distribution than Y-cells. These differences, however, appear to represent tendencies rather than invariant properties and may not be necessary correlates of the type of spatial summation. The results indicate that both groups project to the lateral geniculate body. This projection agrees with the results of anatomical studies (5, 6), which also support the broader overlap of lateral projections across the vertical meridian than the one expected on the basis of earlier studies (24). Similar types of cell have, of course, already been reported in the lateral geniculate body (27). Recent geniculate studies (14, 21) agree to some extent on the existence of a "sustained-slow/transient-fast" dichotomy organized along X-like and Y-like lines that resembles the X/Y dichotomy of ganglion cells. There is some disagreement in relation to the degree of segregation of such X-like and Y-like cells in the various layers (14, 21), although peroxidase-tracing studies of the central projections of small, medium, and large ganglion cell bodies (which should bear on classifications based on conduction velocity) suggest absence of total segregation (6). The original X/Y linearity criterion, however, apparently has not yet been used for the detailed study of geniculate and cortical neurons of macaques. In contrast to the retinogeniculate projection, the retinocollicular one seems to be mediated exclusively by nonopponent-color Y-cells either with or without a center-surround organization (8, 23).

The properties of these three concentrically organized types of macaque ganglion cells indicate the existence of at least three overlapping dichotomies based on the polarity of center responses and on the degrees of spectral opponency and of linearity of spatial summation. Type I and type III cells appear to be the more common ganglion cell types and most of their functional properties, respectively, resemble those reported for human central and peripheral vision, suggesting that many of the functional properties of the visual system of primates may be substantially defined at the level of its ganglion cells. Although type IV cells have some rather unique characteristics (red-sensitive surrounds, apparent absence of off-centers), they seem to have an intermediate and less defined position since some of their properties (spectral opponency, central retinal distribution, frequent input from blue-sensitive cones, absence of collicular projections) resemble those of type I cells, whereas other properties (nonlinear spatial summation, larger receptive fields, short conduction latency, mixing of cone inputs) resemble those of type III cells. From this point of view, type IV cells may perhaps represent an attempt of "fovealization" of the Y-cell system of macaques.

ACKNOWLEDGMENT

I thank Dr. Christina Enroth-Cugell for discussion of the results.

Present address of author: Clinical Branch, National Eye Institute, National Institutes of Health, Bethesda, Md. 20014.

REFERENCES

1. ARDEN, G. B. The retina—neurophysiology. In: *The Eye*, edited by H. Davson. New York: Academic, 1976, vol. 2A, p. 229–356.
2. BARLOW, H. B., FITZHUGH, R., AND KUFFLER, S. W. Change of organization in the receptive fields of the cat's retina during dark adaptation. *J. Physiol. London* 137: 338–354, 1957.
3. BOYCOTT, B. B. AND DOWLING, J. E. Organization of the primate retina: light microscopy. *Phil. Trans. Roy. Soc. London Ser. B* 255: 109–184, 1969.
4. BRINDLEY, G. S. The summation areas of human colour-receptive mechanisms at increment threshold. *J. Physiol. London* 183: 497–500, 1954.
5. BUNT, A. H., MINCKLER, D. S., AND JOHANSON, G. W. Demonstration of bilateral projection of the central retina of the monkey with horseradish peroxidase neuronography. *J. Comp. Neurol.* 171: 619–630, 1977.
6. BUNT, A. H., HENDRICKSON, A. E., LUND, J. S., Lund, R. D., AND FUCHS, A. F. Monkey retinal ganglion cells: morphometric analysis and tracing

of axonal projections, with a consideration of the peroxidase technique. *J. Comp. Neurol.* 164: 265–286, 1975.

7. DE MONASTERIO, F. M. Center and surround mechanisms of opponent-color X and Y ganglion cells of retina of macaques. *J. Neurophysiol.* 41: 1418–1434, 1978.
8. DE MONASTERIO, F. M. Properties of ganglion cells with atypical receptive-field organization in retina of macaques. *J. Neurophysiol.* 41: 1435–1449, 1978.
9. DE MONASTERIO, F. M. AND GOURAS, P. Functional properties of ganglion cells of the rhesus monkey retina. *J. Physiol. London* 251: 167–195, 1975.
10. DE MONASTERIO, F. M., GOURAS, P. AND TOLHURST, D. J. Trichromatic colour opponency in ganglion cells of the rhesus monkey retina. *J. Physiol. London* 251: 197–216, 1975.
11. DE MONASTERIO, F. M., GOURAS, P., AND TOLHURST, D. J. Concealed colour opponency in ganglion cells of the rhesus monkey retina. *J. Physiol. London* 251: 217–229, 1975.
12. DE MONASTERIO, F. M., GOURAS, P., AND TOLHURST, D. J. Spatial summation, response pattern and conduction velocity of ganglion cells of the rhesus monkey retina. *Vision Res.* 16: 674–678, 1976.
13. DE VRIES, H. L., SPOOR, A., AND JIELOF, R. Properties of the eye with respect to polarized light. *Physica* 19: 419–432, 1953.
14. DREHER, B., FUKADA, Y., AND RODIECK, R. W. Identification, classification and anatomical segregation of cells with X-like and Y-like properties in the lateral geniculate nucleus of old-world primates. *J. Physiol. London* 258: 433–452, 1976.
15. ENROTH-CUGELL, C. AND PINTO, L. H. Properties of the surround response mechanism of cat retinal ganglion cells and centre-surround interaction. *J. Physiol. London* 220: 403–439, 1972.
16. ENROTH-CUGELL, C. AND ROBSON, J. G. The contrast sensitivity of retinal ganglion cells of the cat. *J. Physiol. London* 187: 517–552, 1966.
17. GOURAS, P. Identification of cone mechanisms in monkey ganglion cells. *J. Physiol. London* 199: 533–547, 1968.
18. HOCHSTEIN, S. AND SHAPLEY, R. M. Quantitative analysis of retinal ganglion cell classification. *J. Physiol. London* 262: 237–264, 1976.
19. HOLDEN, A. L. The central visual pathways. In: *The Eye*, edited by H. Davson. NewYork: Academic, 1976, vol. 2A, p. 357–474.
20. KUFFLER, S. W. Discharge patterns and functional organization of mammalian retina. *J. Neurophysiol.* 16: 37–68, 1953.
21. MARROCCO, R. T. Sustained and transient cells in monkey lateral geniculate nucleus: conduction velocities and response properties. *J. Neurophysiol.* 39: 340–353, 1976.
22. POLYAK, S. L. *The Retina*. Chicago: University Press, 1941.
23. SCHILLER, P. H. AND MALPELI, J. G. Properties and tectal projections of monkey retinal ganglion cells. *J. Neurophysiol.* 40: 428–445, 1977.
24. STONE, J., LEICESTER, J., AND SHERMAN, S. M. The naso-temporal division of the monkey's retina. *J. Comp. Neurol.* 150: 333–348, 1973.
25. TOYODA, J. Frequency characteristics of retinal neurons in the carp. *J. Gen. Physiol.* 63: 214–234, 1974.
26. WESTHEIMER, G. The Maxwellian view. *Vision Res.* 6: 669–682, 1966.
27. WIESEL, T. M. AND HUBEL, D. H. Spatial and chromatic interactions in the lateral geniculate body of the rhesus monkey. *J. Neurophysiol.* 29: 1115–1156, 1966.